Electrochimica Acta 476 (2024) 143708

Contents lists available at ScienceDirect

Electrochimica Acta

journal homepage: www.journals.elsevier.com/electrochimica-acta

Assessment of *in-vivo* corrosion of Ti and CoCrMo joint implants by electrochemical measurements in human synovial liquids

Yueyue Bao [a], Anna Igual Muñoz [a,*], Brigitte M. Jolles [b,c], Stefano Mischler [a]

[a] *École Polytechnique Fédérale de Lausanne, Lausanne CH-1015, Switzerland*
[b] *Swiss BioMotion Lab, Lausanne University Hospital and University of Lausanne (CHUV-UNIL), Lausanne CH-1011, Switzerland*
[c] *Institute of Electrical and Micro Engineering, Ecole Polytechnique Fédérale de Lausanne (EPFL), Lausanne CH-1015, Switzerland*

ARTICLE INFO

Keywords:
Human synovial fluids
Corrosion
Ti
CoCrMo
Galvanic corrosion
Tribocorrosion

ABSTRACT

Understanding the corrosion behavior of biomedical materials in the human body is an essential step for the development of improved materials and clinical procedures in arthroplasty. In this work, the corrosion behavior of Ti and CoCrMo alloys in human synovial fluids directly extracted from patients was investigated through an electrochemical experimental protocol, including open circuit potential (OCP), electrochemical impedance spectroscopy (EIS) and potentiodynamic polarization measurements. The results show that the corrosion behavior of both materials largely depends on patients. The obtained corrosion rates of both materials correspond well to the metal ion release rate detected in patients with joint implants revealing the adequateness of the electrochemical experimental protocol for quantifying *in-vivo* corrosion of biomedical implants. Based on the results, no significant risk of galvanic corrosion of Ti/CoCrMo coupling is anticipated. The rates of wear-accelerated corrosion (one of the main degradation mechanisms of metallic artificial hip joints) were theoretically extracted from the present electrochemical measurements using an established tribocorrosion model. Those material loss rates are patient-dependent and can be up to two orders of magnitude higher than the static corrosion rates, indicating that the nature of the patient can critically affect the degradation rate of the joint implant.

1. Introduction

Along with the rapid modern medical development, the application of biomedical devices has been continuously increasing in recent years. By 2030, knee joint arthroplasty in the USA is estimated to be about 3000,000 cases [1]. The lifetime of implants was associated with the release of metal ions into the human body by corrosion of the implants, which above a patient-dependent critical threshold [2], can become harmful to the human body [3–5].

To improve the performance of implant materials, it is essential to understand the corrosion behavior of implant materials in the human body. So far, corrosion of alloys used for orthopedical implants (typically Ti and CoCrMo alloys) was mainly investigated in simulated body fluids, including isotonic sodium chloride (NaCl) [6–10], phosphate buffers (PBS) [6,7,11–13] and the more complex Hank's [7–9,14] solutions. Bovine serum albumin (BSA) [11–13,15] and hyaluronic acid [9,14] are sometimes added to simulate the effect of organics. Besides, hydrogen peroxide (H_2O_2) [10,13,16] is introduced to mimic the body's inflammation conditions. These studies reveal that the corrosion reaction between metals and human synovial fluids depends on a large number of complex phenomena. For instance, phosphate and calcium ions slightly diminish the anodic current of CoCrMo alloy [6,11] and Ti alloy [7,8,17] by adsorbing onto the metal surface. BSA can inhibit the reduction reactions by adsorbing onto the metal surface [6,11]. However, depending on the concentration, protein can either accelerate the corrosion rate of metals by forming soluble complexes with metal ions [11,13] or inhibit corrosion by acting as a physical barrier [11,15]. The impact of HA on the corrosion behavior of Ti [14] and CoCrMo alloy [9] is limited compared with BSA due to its hydrophilic property and large size that lead to less adsorption on the metal surface. In addition, H_2O_2 can significantly increase the corrosion rate of the metal [10,13,16] owing to the unpaired electrons in the valence shell. However, the effect of each phenomenon was only studied independently, and their application to complex human body fluids has not been well validated.

The study of electrochemical reactions of metal directly in human synovial fluids is quite limited [18–21]. Munoz et al. [18] investigated

* Corresponding author.
E-mail address: anna.igualmunoz@epfl.ch (A.I. Muñoz).

https://doi.org/10.1016/j.electacta.2023.143708
Received 5 December 2023; Received in revised form 21 December 2023; Accepted 21 December 2023
Available online 23 December 2023

the electrochemical behavior of a CoCrMo alloy in different synovial fluids, which were directly extracted from 17 patients with different clinical states. The results show that the electrochemical behavior of the alloy varied significantly with the various synovial fluids. Besides, a significant difference between *in-vivo* and *in-vitro* corrosion behavior was obtained, probably due to the complex composition of synovial fluids. Similarly, the patient-dependent corrosion behavior of Ti in human synovial fluids was also reported in [21], where the *in-vivo* results cannot be explained by the *in-vitro* ones. Besides electrochemical research, retrieved prostheses are investigated to study the actual reaction behavior of metal in synovial fluids. Different surface layers, from oxide film to organic or graphitic film, were found on retrieved implant load-bearing surfaces [22–24]. However, only the case of an oxide film underneath an organic layer is reported in the *in-vitro* research [25,26]. These results indicate that *in-vitro* experiments do not necessarily represent the whole *in-vivo* behavior.

It is therefore necessary to investigate the corrosion behavior of metal in real human synovial fluids to determine the actual reaction behavior and predict the lifetime of the implants. In our previous work [21], a novel short-term electrochemical experimental protocol has been designed and validated to assess the corrosion behavior of Ti in synovial fluid directly extracted from patients. This study revealed that the electrochemical response of Ti is highly dependent on the patient. Comparison with *in-vitro* experiments using the same protocol evidenced that the main difference lies in the cathodic response linked to the presence in the synovia of organic compounds and the activity of dissolved oxygen.

In this study, the novel electrochemical experimental protocol [21] was applied to a new cohort of patients to investigate the corrosion behavior of Ti and CoCrMo alloy both materials immersed in the same human synovial fluid. The pertinence of the electrochemically determined corrosion rates will be appraised by comparison with the metal ion release rates measured in patients with orthopedic implants. This allows to assess relevant clinical implications, such as the risk of galvanic corrosion in implants combining Ti or Ti alloys with CoCrMo alloys. Moreover, the obtained electrochemical measurements will be exploited to evaluate through a tribocorrosion model the risk of damage of artificial hip joints as a function of the patient.

2. Experimental

2.1. Materials

A Ti rod (grade 2: Ti $\geq$ 98.9 wt.%, Fe $\leq$ 0.30 wt.%, $O \leq$ 0.25 wt.%, C $\leq$ 0.08 wt.%) and a low carbon CoCrMo alloy rod (Co: 65.95 wt.%, Cr: 28 wt.%, Mo: 6 wt.%, C: 0.05 wt.%) supplied by Goodfellow were used in this study. Samples were cut from bulk rods with a diameter of 4 mm and a thickness of 6 mm. The samples were polished with SiC emery paper from 1200 to 4000 grit in water, followed by a polish tissue with an ethanol-based diamond suspension (0.25 μm in diameter). The final surface roughness (Ra) was measured by a laser scanning confocal microscope (KEYENCE VK-X200), and the value for Ti and CoCrMo alloy was 15 $\pm$ 3 nm and 10 $\pm$ 1 nm, respectively. The Ra value of CoCrMo alloy is the typical surface roughness for artificial joints. Afterwards, the samples were cleaned in acetone and 70 % ethanol with ultrasonics for 5 min, respectively, following the dry-up with oil-free compressed air.

A multi-electrode cell with a 2 ml volume was used for the electrochemical measurements, as shown in the previous paper [21]. Two Ti and two CoCrMo samples, serving as working electrodes (WE), were placed in the cell and tested under the same conditions. Besides, an Ag/AgCl (3.5 M KCl) electrode and platinum rods were used as reference electrode (RE) and counter electrodes (CE), respectively.

The synovial fluids were extracted from patients by a skilled surgeon with a syringe. Contamination of synovial fluids by blood or other components was minimized. The extraction procedure is explained in detail in [21]. The overall protocol of this study (protocol 208/13) was approved on 28 May 2013 by the ethics committee for human being studies of the local government (Commission cantonale (VD) d'éthique de la recherché sur l'être humain) according to the ICH GCP guidelines. Note that for legal reasons, no access to clinical information concerning the patients was permitted to nonmedical staff.

The fluids were directly transferred to the electrochemical laboratory within 5 min. The picture of synovial fluid was taken right after. Subsequently, the pH of the fluid was measured with pH paper (sensitivity is 0.3 pH units) by depositing a drop of synovia from the syringe onto the paper. Ultimately, synovial fluids were injected into the cell until complete filling. The liquids were also subjectively categorized during the injection into the electrochemical cell according to their consistency in sticky (similar to glycerol) or liquid (similar to vegetable oil). The measurements were carried out at 37 $\pm$ 1 °C. The detailed experimental procedure is described in [21].

2.2. Electrochemical experiments

Different electrochemical measurements were conducted sequentially on the samples using a potentiostat IVIUM VERTEX:

- The OCP of 10 Platinum rods (2 diameter) and a Ag/AgCl reference electrode (RE) was measured for 10 s sequentially. The standard deviation of the OCP-CE values (STDEV) was used for assessing the degree of homogeneity of synovial fluids. The Pt rods were short-circuited to act as a counter electrode in the following electrochemical tests.
- The OCP between 4 working electrodes made of titanium and CoCrMo alloys (WE) and the RE was measured during 5 mins.
- The Polarization resistance (Rp) of one of the Ti and one of the CoCrMo was conducted after the OCP measurement by applying a potential $\pm$ 20 mV with respect to OCP with a scan rate of 2 mV/s.
- The second and third steps were repeated four times.
- The solution resistance (Rs) was obtained by carrying out an Electrochemical Impedance Spectrosocpy test (EIS) on the same Ti and CoCrMo samples at the OCP. The applied potential amplitude was $\pm$10 mV and the frequencies were scanned from 10^5 to 1 Hz.
- Potentiodynamic scans were conducted on the same Ti and CoCrMo sample by scanning the potential from the OCP to -1 $V_{Ag/AgCl}$ and reversing it to 1 $V_{Ag/AgCl}$ with a scan rate of 2 mV/s.
- The Rs was measured again at the end of the sequence by the EIS procedure on the Ti and the CoCrMo samples.

The whole experiment procedure is shown in Fig. 1.

3. Results

3.1. Human synovial fluids

67 patients (patient number 20 to 86) were tested among which only 22 patients had enough amount of synovial liquid ($\geq$ 2 ml) to carry out the electrochemical measurements. The information of the tested synovial fluids is summarized in Table 1. The pH of the extracted synovia varies from 6.5 to 8.2 although most of the samples lied around 7.3. The maximum pH change after the electrochemical tests was of 0.5 units. As already previously reported for patient number 2 to 18 [21], the color of the synovial liquids was yellow or red, depending on the patient while the qualitatively aspect of the synovia was liquid, sticky (similar to glycerol) or little sticky (similar to vegetable oil). The measurement of the OCP of the individual Pt wires was used to assess the electrochemical homogeneity of the synovial fluid [21]. The standard deviation of the measured OCP values varies depending on the patient, from 12 mV to 49 mV. These values are very close to those found in 0.8 % NaCl solution (32 mV), indicating that the synovial fluids are homogeneous.

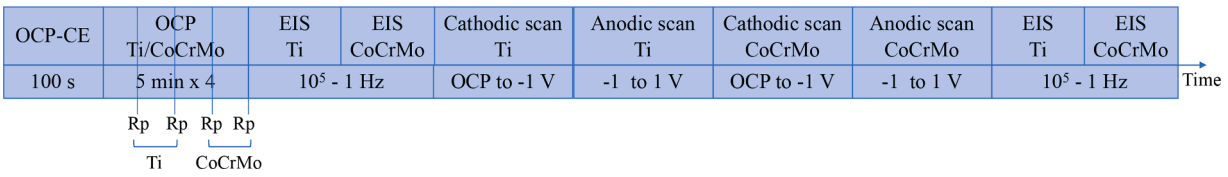

Fig. 1. Experimental electrochemical sequence followed to test Ti and a CoCrMo alloy in the synovia extracted from patients.

Table 1
Properties of human synovial fluids extracted from tested patients.

Patient number	Volume/ml	pH	Observation
20	6	8.2	Sticky
21	6	7.9	Sticky
22	6	7.9	Sticky
23	7	7.6	Sticky
26	4	7.9	Little sticky
28	6	7.6	Little sticky
31	4	7.9	Sticky
35	6	7.6	Little sticky
36	6	7.6	Liquid
39	8	7.3	Liquid
43	7	7.3	Sticky
46	8	7.3	Liquid
48	10	7.0	Sticky
53	6	7.3	Liquid
59	5	7.6	Sticky
71	8	7.3	Little sticky
73	3	7.3	Little sticky
75	2	8.0	Little sticky
76	5	6.5	Liquid
78	6	7.3	Liquid
83	6	7.0	Sticky
86	2	n.d.	Sticky

3.2. OCP of Ti and CoCrMo alloy

The OCP of the two Ti and two CoCrMo alloy samples was measured sequentially every 5 min. Fig. 2 illustrates three examples of those measurements showing the different OCP variations with time for both materials. For most patients, the OCP values of the two tested electrodes stabilized after 10–15 min of immersion, as observed for patient P21. However, exceptions are observed in CoCrMo. For example, patient P73 exhibits a decreasing trend of OCP of both CoCrMo electrodes, while an increasing trend was observed for P22 on one electrode only.

The final OCP of Ti and CoCrMo alloy measured after 20 min of immersion in the tested synovia is shown in Fig. 3. The final OCP of Ti varies with patients between a minimum of −560 $mV_{Ag/AgCl}$ and a maximum of −230 $mV_{Ag/AgCl}$. Like Ti, the final OCP of the CoCrMo sample depends on patients, varying from −500 $mV_{Ag/AgCl}$ to −300 $mV_{Ag/AgCl}$. Similar values between the two tested Ti electrodes and the two CoCrMo samples were obtained except for P21, P59, P71 and P83 for Ti and P22 and P48 for CoCrMo. The OCP values of Ti can be higher or lower than that of CoCrMo alloy, depending on the synovial fluid.

It is worth noting that the sterilization methods influence the OCP values. For instance, higher OCP values ranging from −83 $mV_{Ag/AgCl}$ to 0 $mV_{Ag/AgCl}$ were obtained for CoCrMo alloy in a previous study before being tested [18], where the samples were sterilized in an autoclave under saturated steam at 121° for 20 min. This is due to the changes in the passive film thickness and composition which accelerates the oxygen reduction reaction and inhibits the anodic dissolution [27]. A thicker and Cr-rich passive film was formed on the CoCrMo surface sterilized in an autoclave compared to the one obtained when the sterilization was done in 70 % ethanol, as in the present work.

3.3. Rp of Ti and CoCrMo alloy

Examples of Rp measurements for Ti and CoCrMo alloy are shown in Fig. 4. For both materials, a linear variation of current with applied potential is not observed across the zero current due to the capacitive effects of the double layer and passive film. These results correspond to those previously reported [21]. Nevertheless, Rp values were determined by taking the reciprocal of the slope of the linear part in the anodic region of the i vs E plots.

The obtained Rp values for Ti and CoCrMo alloy tested in the different synovia from patients are shown in Fig. 5. These results show a significant variability in the Rp of Ti among patients, up to 50-fold difference, with P46 showing the highest and P20 the lowest Rp. Analogously, the Rp of the CoCrMo alloy varies among patients, with a notable difference up to 70-fold. The highest Rp value was obtained for P48 and the lowest for P20. Besides, the results reveal that much higher

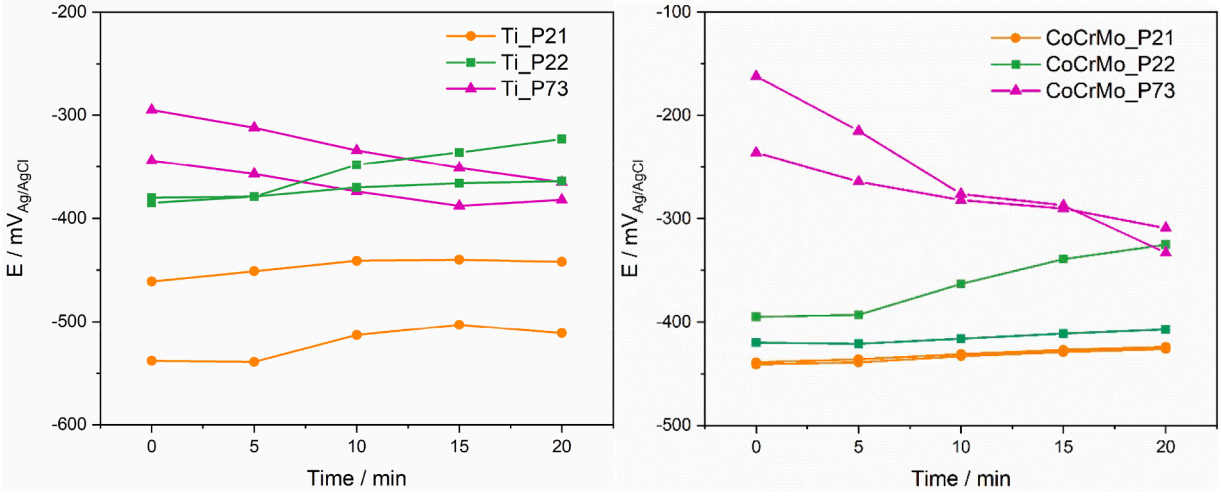

Fig. 2. OCP variation with the immersion time of Ti and CoCrMo samples in different synovial fluids. The potentials of the two Ti and the CoCrMo electrodes are shown for each patient.

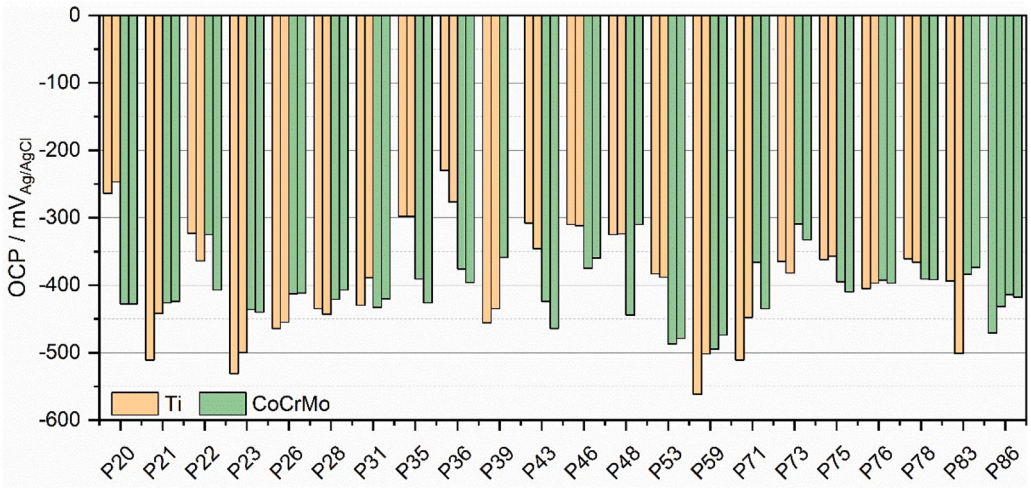

Fig. 3. OCP values after 20 min of immersion of Ti and CoCrMo alloy in different synovial fluids.

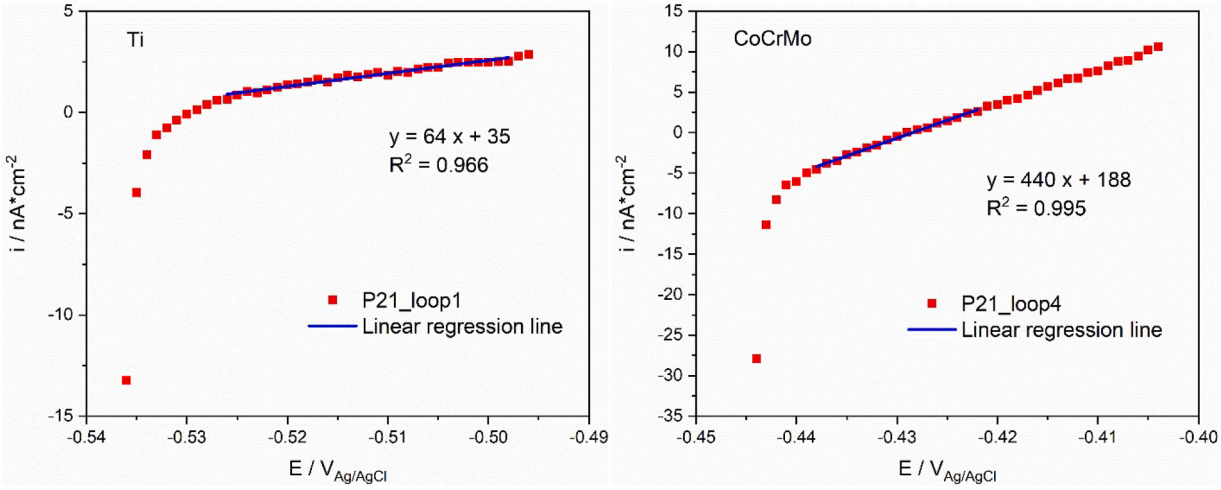

Fig. 4. Examples of Rp measurements of Ti and CoCrMo alloy in synovial fluid from P21.

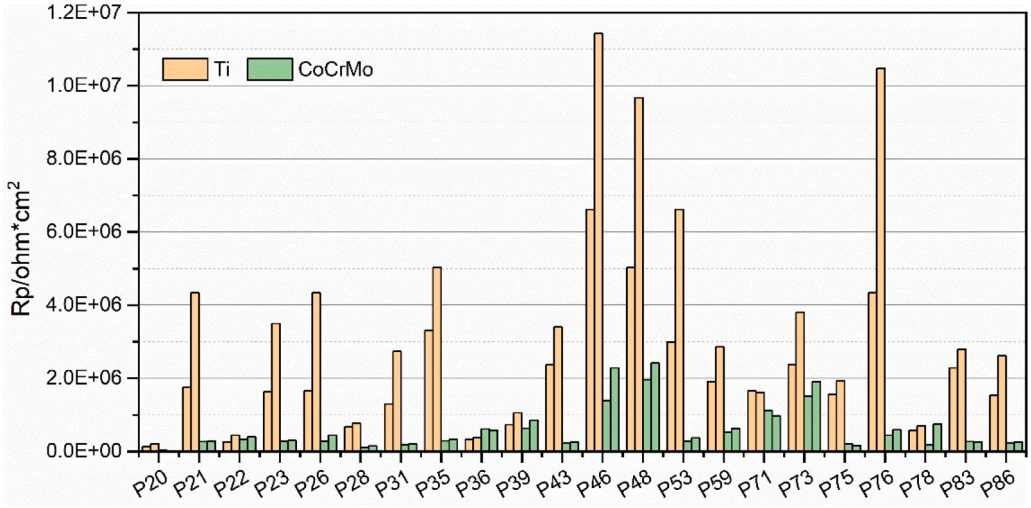

Fig. 5. Rp value of Ti and CoCrMo alloy in all synovial fluids.

Rp values are obtained for Ti compared with CoCrMo alloy in most of the synovial fluids (from a minimum of 10 KOhm*cm^2 for P39 to a maximum of 7 MOhm*cm^2 for P46.). The only exception was found for P22 and P36, in which the Rp value of both materials are very close.

3.4. Conductivity of synovial fluids

The solution resistance (Rs) of the synovial fluid, inversely proportional to its conductivity, was extracted from the impedance spectra at a frequency of 10^5 Hz. The Rs values of the different synovial fluids are shown in Fig. 6. The solution conductivity was acquired based on the distance between the RE and the WE, the Rs and the surface area of the WE. The values of the conductivity of each synovial fluid are shown in form of dashed bars in Fig. 6. The results indicate that synovial fluids are conductive and present a resistance similar to the 0.8 % NaCl solution (80 Ohm which corresponds to 1.8 S/m). Besides, no significant difference in the Rs tested before and after the potentiodynamic scan was observed, thus suggesting that the scan does not significantly modify the conductivity of the synovial fluids.

3.5. Potentiodynamic polarization curves of Ti and CoCrMo alloy

The representative cathodic and anodic polarization curves of Ti in the synovial fluids are shown in Fig. 7a and 7b, respectively. All polarization curves in all tested synovia are shown in the supplementary material (Figs. S1, S2). Fig. 7a shows that the cathodic current density varies more than two orders of magnitude depending on the patient. Patients P20 and P26 exhibit exceptionally high current densities. All curves show a linear part around 100 - 200 mV below the OCP.

Three potential domains are observed in the anodic polarization curves, Fig. 7b: the cathodic domain below the corrosion potential (E_{cor}), where the current density is dominantly determined by the reduction reaction, the cathodic/anodic transition at $E_{cor,}$ and the passive domain at higher potentials. The passive domain is typically characterized by an initial steady increase in current followed by a current plateau. The passive domain of the polarization curves of P20, P28 and P31 (supplementary material) exhibit current oscillations, whose origin is not clear at this moment.

The cathodic and the anodic polarization curves of the CoCrMo alloy are plotted in Fig. 8a and 8b. The results for the overall series of patients are reported in the supplementary material (Figs. S3, S4). Contrary to the Ti, the cathodic current densities of the CoCrMo alloy are quite similar among patients, except in P20 where higher cathodic and anodic currents are observed, as shown in Table S2 (supplementary material). All curves exhibit two linear parts: around the region from −0.4 to −0.7 $V_{Ag/Ag/Cl}$ and from −0.85 to −1 $V_{Ag/Ag/Cl}$.

Four potential domains are observed in the anodic polarization curves of the CoCrMo, Fig. 8b: the cathodic domain below the corrosion potential (E_{cor}), the cathodic/anodic transition at $E_{cor,}$ the passive domain within the current plateau and the transpassive domain where the current increase with potential. The anodic polarization curves, as in the case of the cathodic ones, exhibit slight differences (within one order of magnitude) among patients.

It is worth noting that the two polarization curves measured on two Ti samples for P79 and two CoCrMo alloys for P85 exhibit very similar behavior, as shown in the supplementary material. This good repeatability confirms the pertinence of electrochemical measurements in the synovial fluids.

To quantitatively assess the electrochemical behavior of both materials, characteristic parameters are extracted from the cathodic polarization curves of the Ti and the CoCrMo alloy, and they are listed in Table 2. The Tafel constant b_c is obtained as the reciprocal of the slope of the linear part immediately below E_{cor*}. The corrosion potential E_{cor*} equals the OCP of Ti and CoCrMo alloy. The corrosion current density i_{cor} was obtained by extrapolating the linear part of the logarithmic plots displayed in Figs. 7a and 8a to the OCP value.

Table 2 shows that the b_c varies among patients, with a range from 83 to 385 mV for Ti and from 117 to 267 mV for CoCrMo alloy. These variations suggest differences in the mechanisms of the cathodic reduction reaction [28]. Similarly, depending on the patient, the i_{cor} values of Ti vary from 0.02 to 0.5 μA/cm^2. For CoCrMo alloy, the i_{cor} values range between 0.02 and 6 μA/cm^2, and most values lie in the narrow range of 0.2 to 0.1 μA/cm^2.

4. Discussion

4.1. Electrochemical reactions of Ti and CoCrMo alloy in synovial fluids

As shown in Figs. 7, S1 and S2, the electrochemical behavior of Ti is patient-dependent, especially with respect to the cathodic reactions. The reversible potentials of oxygen and hydrogen reduction reactions at a pH 7 and 37 °C are 0.6 $V_{Ag/agCl}$ and −0.6 $V_{Ag/AgCl}$, respectively. This implies that in the studied cathodic domain, the reduction of dissolved oxygen ($E \leq$ OCP), water and protons ($E \leq -0.6$ $V_{Ag/AgCl}$) occur. The cathodic reduction depends on many factors [11,13], such as the concentration of reactants, the electrode surface state (nature of passive film, adsorption of organics and ions) and the potential. It is therefore not straightforward to attribute the significant differences in cathodic kinetics

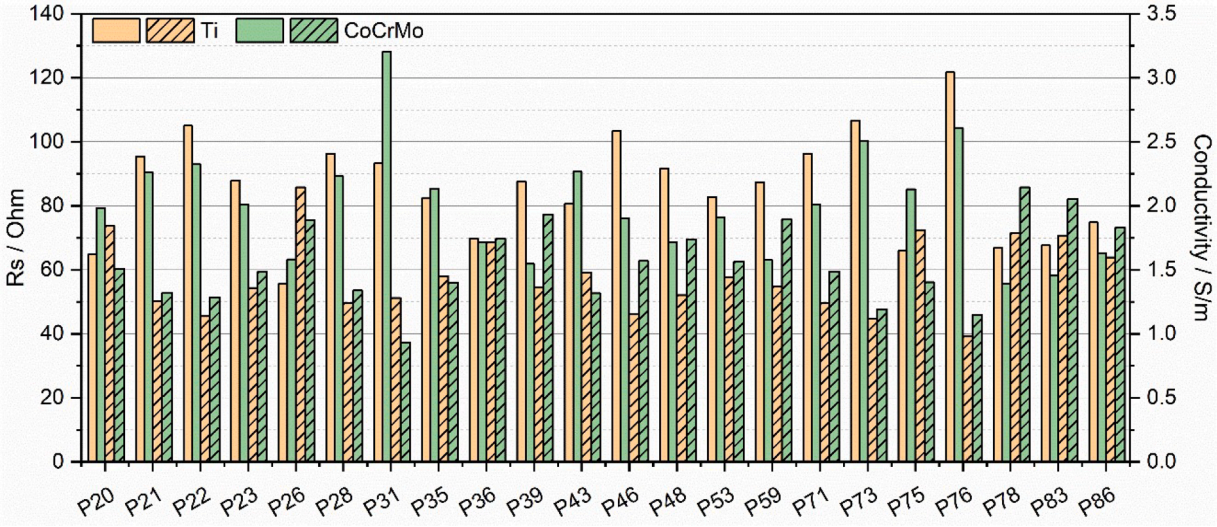

Fig. 6. Solution resistance and conductivity of synovial fluids from different patients.

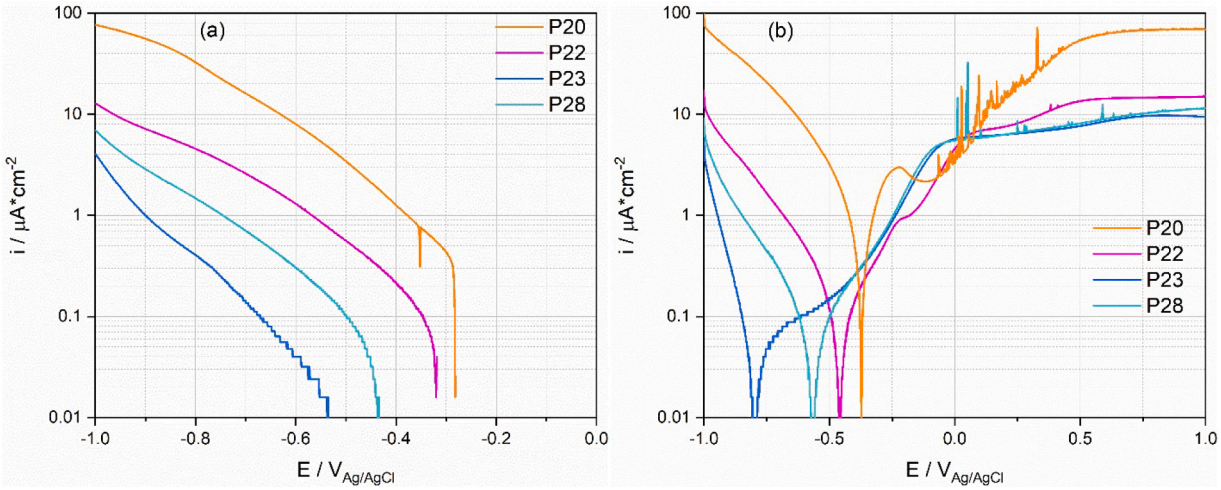

Fig. 7. (a) Cathodic and (b) anodic polarization curves of Ti in several synovial fluids.

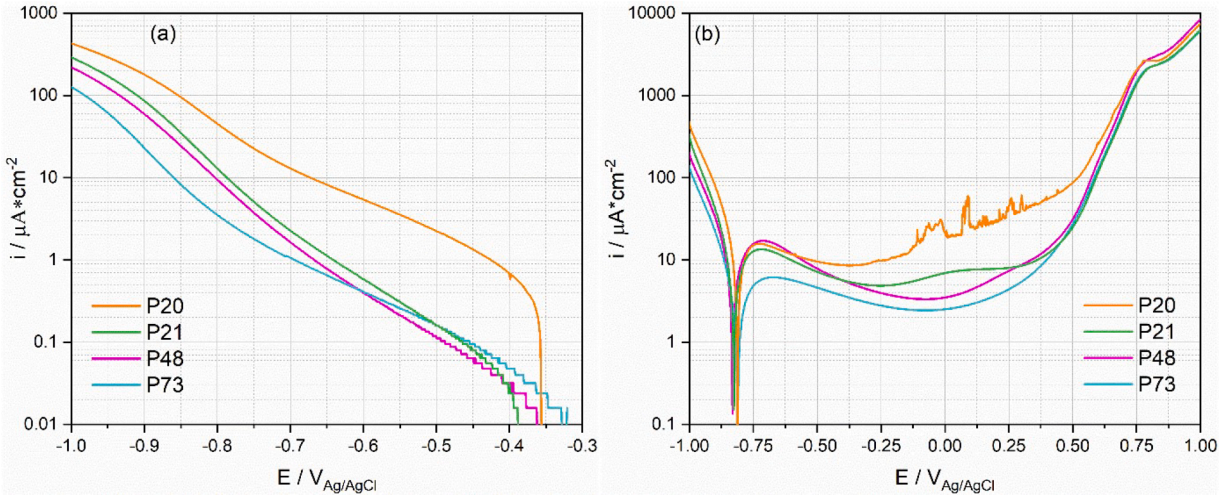

Fig. 8. (a) Cathodic and (b) anodic polarization curves of CoCrMo tested in synovial fluids.

observed on Ti (Fig. 7a) to specific factors. One can only argue that since the pH of tested synovial fluids little varied among patients (Table 1), the role of proton reduction appears marginal. Indeed, comparison with *in-vitro* studies allowed to identify the concentration of dissolved oxygen and organic adsorption as crucial factors affecting the cathodic kinetics of Ti in synovial fluids [8,13].

In the anodic domain, the polarization curves of the patients follow a similar trend up to 0 V_{AgAgCl} characterized by a steady increase in the current. Above this potential, the plateau current may differ significantly depending on the patient. The origin of the plateau is probably linked to the transition from the oxidation of Ti to Ti_2O_3 and to the thermodynamically more stable TiO_2 [28–30]. The passive current density is determined by the rate of passive film growth and the film dissolution kinetics. The synovial fluid chemistry can interfere in a complex way with both mechanisms. For example, organic molecules can promote film dissolution by forming complexes with the metal ions released from the passive film. On the other hand, protein can adsorb on the passive film surface and inhibit passive film dissolution [9,12,31].

Similarly, the cathodic current for CoCrMo alloy is also determined by the reduction of dissolved oxygen, water and protons. It depends therefore on the same factors as mentioned above for Ti.

The anodic part of the polarization curves of CoCrMo are characterized by a passive plateau followed, at higher potential, by a transpassive domain. The passive film on CoCrMo mainly consists of Cr_2O_3/$Cr(OH)_3$ and smaller amounts of Co oxide/hydroxide and Mo oxide/hydroxide [32,33]. As discussed for Ti, the passive current density is governed by the passive film growth and its dissolution. The variation of passive current density could then depend on the protein concentration [34] as protein can either interact with the metal ions by forming soluble complexes (increase the dissolution rate of the film) or adsorb on the metal surface, inhibiting the dissolution process [6,11]. The passive current density could also be influenced by the ions in the synovial fluids. For instance, it is reported that phosphate ions adsorb on the sample surface, enhancing the passive dissolution resistance [35]. In addition, current oscillations were observed in three patients, two of which showed also the presence of isolated cells on the tested surfaces. Therefore, those currents oscillation could be attributed to the local presence of cells on the titanium surfaces. The SEM images of the Ti sample surface after exposure in synovial fluids for P11 and P20 are shown in Fig. S5 (supplementary material).

In the transpassive domain, the current starts to increase with applied potential due to the transformation of Co(II), Cr(III) and Mo(IV) oxide to Co(III), Cr(VI) and Mo(VI) oxide, as well as oxidation of water. The latter two oxides are soluble, resulting in the dissolution of the passive film. The transpassive current may be affected by the presence of protein and phosphate ions, which react with metallic ions by forming complexes and thus enhance dissolution [35].

Table 2
Electrochemical parameters extracted from the cathodic polarization curves of Ti and CoCrMo alloy.

Patient	Ti			CoCrMo alloy		
	b_C / mV	E_{cor*} / $mV_{Ag/Ag/Cl}$	i_{cor} /μA/ cm^2	b_C / mV	E_{cor*} / $mV_{Ag/Ag/Cl}$	i_{cor} /μA/ cm^2
20	237	−247	0.2	267	−428	0.6
21	99	−442	0.02	147	−424	0.04
22	304	−364	0.1	145	−407	0.04
23	101	−500	0.02	134	−440	0.05
26	111	−455	0.02	143	−412	0.06
28	276	−443	0.08	147	−407	0.09
31	88	−389	0.04	147	−420	0.08
35	168	−298	0.02	138	−431	0.05
36	343	−277	0.2	193	−426	0.04
39	216	−282	0.04	154	−359	0.03
43	223	−346	0.04	124	−464	0.05
46	85	−312	0.02	164	−360	0.02
48	83	−324	0.02	152	−310	0.02
53	67	−388	0.02	117	−479	0.04
59	74	−502	0.02	120	−474	0.03
71	85	−448	0.02	129	−435	6
73	74	−382	0.5	246	−333	0.03
75	147	−357	0.04	203	−410	0.09
76	71	−397	0.02	170	−397	0.04
78	385	−366	0.1	200	−392	0.1
83	129	−501	0.02	198	−374	0.05
86	92	−432	0.02	184	−418	0.07

4.2. Metal ion release rates of Ti and CoCrMo alloy in synovial fluids

In order to compare the obtained corrosion rates with the metal ion release found *in-vivo*, the i_{cor} (μA/cm^2) were converted into mass loss m_{cor} (mg/dm^2/day^1) through the Faraday's law according to the following equation:

$$m_{cor} = 8640 M i_{cor} / nF \quad (1)$$

Where M is the atomic mass: 48 g/mol (Ti), 59 g/mol (Co), 52 g/mol (Cr) and 96 g/mol (Mo), F is Faraday constant: 96,485 A s/mol and n is its oxidation valence which is assumed to be 4 (Ti), 2 (Co), 3 (Cr) and 4 (Mo).

Although the concentrations of metallic ions in serum, plasma, whole blood, and urine are largely reported in the literature, no information about *in-vivo* corrosion rates of Ti and CoCrMo alloy could be found. Nevertheless, the corrosion rate can be tentatively estimated by considering that, in case of no further ion accumulation in the body, it corresponds to the release rate of metal ions through urine. This is a coarse assumption, as ions can be eliminated through other ways, such as sweat and hair growth [4].

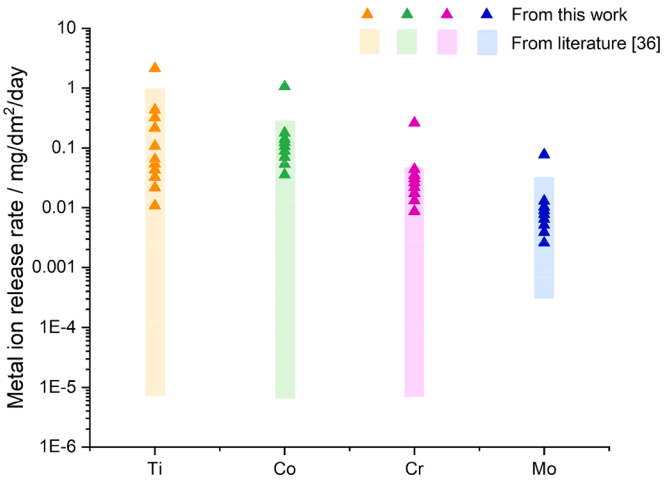

Fig. 9. Comparison of the metal ion release rates (points) obtained from the icor values calculated in this study and those obtained from the literature (bars) [36].

Considering an approximative Ti or CoCrMo exposed hip joint implant surface of 1 dm^2 [21], this yields an elimination rate of Ti/Co/Cr/Mo through urine in the range of 6×10^{-6} mg/dm^2/day to 1.2 mg/dm^2/day, as displayed in Fig. 9. The release rates of Co, Cr and Mo are calculated by assuming the amount of released metal ions is proportional to the bulk alloy composition. Ti/Co/Cr/Mo concentration in urine for patients with hip and knee implants was reported by Matusiewicz [36]. Given that the typical urine release rate of human bodies is approximately 1.5 l per day, the measured metal ion release rates are displayed in Fig. 9. This range corresponds well to the corrosion rates obtained in this study. It is worth noting that the metal ion release rates obtained from this study are in the upper limit of those found in the literature. This can be due to the fact that the values tested in urine are only a fraction of the overall metal ion release, as well as the fact that the corrosion rates usually decrease with time.

The good correlation between these electrochemical corrosion rate measurements in synovial fluid and the overall metal release rates detected in patients opens the perspective of using the short *in-vivo* protocol used in this study to anticipate the patient response to a given implant material. As a preliminary step, the patients whose synovial fluid was characterized using our protocol, should be followed surgery regarding metal content in the urine. In this way, a quantitative correlation between electrochemical measurements and effective metal release rate could be confirmed.

4.3. Galvanic corrosion between Ti and CoCrMo alloy in human synovial fluids

Ti/CoCrMo coupling is widely used in joint prostheses, for example, in hip implants with a CoCrMo head inserted into a femoral stem made from Ti or Ti alloy. The contact of dissimilar materials in an environment can result in galvanic corrosion because of the possible differences in electrode potentials.

In this work, the risk of galvanic corrosion is determined by quantifying the galvanic current density of Ti and CoCr tested in synovial fluids. The galvanic current density i_G is the cell current flowing between an imaginary electrode 1 (e.g., Ti) and an electrically connected imaginary electrode 2 (e.g., CoCrMo) immersed in an electrolyte. The galvanic current flows from the electrode with a higher potential (cathode) to the one with the lowest potential (anode). It corresponds to the corrosion enhancement of the anode caused by the coupling with the cathode. The galvanic corrosion between coupling materials in simulated body fluids [37–39] depends on several factors, such as surface state [37], solution composition [38,39] and area ratio [28]. For instance, pure Ti behaves as an anode when coupled to CoCrMo alloy in saline solutions, while it has a cathodic behavior after an acid etching surface treatment [37].

The galvanic current density was calculated from the OCP and Rp values of Ti and CoCrMo as tested in synovial fluids using Eq. (2) [28]:

$$i_G = \frac{OCP_c - OCP_a}{R_c + R_a + Rs + Rext} \cdot \frac{1}{A_a} \quad (2)$$

$$i_G = \frac{OCP_c - OCP_a}{Rp_c + Rp_a} \quad (3)$$

Where OCP_c and OCP_a represent the OCP (mV) of the two materials acting as cathode and anode, respectively. Rc and Ra represent the polarization resistance (Ohm) of the two materials in the electrolytes. Rs represents the solution resistance (Ohm) between the two materials, and R_{ext} represents the resistance of the electronic conductors (Ohm), which is not considered due to the negligible electrical resistance. A_a represents the surface area of the anode (cm^2).

Taking into account the surface areas of both electrodes, Eq. (2) can be rewritten as Eq. (3), where Rp_c and Rp_a are the polarization resistance values of both materials obtained from Fig. 5. The solution resistance of the tested synovial fluid can be neglected since its value is much lower than that of Rp.

By using the values in Fig. 3 (for the OCPs) and Fig. 5 (for the Rps), the galvanic corrosion of the Ti/CoCrMo coupling in the different synovial fluids was obtained and plotted in Fig. 10. In the graph, the green bars show that CoCrMo alloy acts as the anode. i_G varies with patients from the nA/cm^2 range to the μA/cm^2 range. The maximum and the minimum iG values were found in P20 and P76, respectively. i_G values are close to the corrosion current densities of the Ti in the synovial fluids, indicating that the coupling with CoCrMo does not significantly increase the Ti corrosion rates. The i_G values of the CoCrMo are even smaller than its corrosion rates, therefore, no significant galvanic effect is expected for the CoCrMo coupled to Ti. This is probably due to the small differences between the OCPs of Ti and CoCrMo alloy in synovial fluids.

4.4. Tribocorrosion

Apart from corrosion, Ti and CoCrMo joint implants are also subjected to tribological loading, resulting in the combined action of corrosion and wear, namely tribocorrosion. Under this condition, the passive film on the metal surface is removed by the mechanical loading and leads the underneath active metal exposed to the fluids. This can increase the corrosion rate by several orders of magnitude [40], the so-called wear-accelerated corrosion, which is one of the main causes of joint degradation [41]. Under tribocorrosion conditions, a galvanic corrosion cell forms between the worn area (anode) and the non-worn area, which remains passive (cathode). The corrosion rate of the anode i_a can then be estimated from cathodic polarization curves by using a simple model originally developed for the tribocorrosion of aluminum alloys [42] and later validated for Titanium and CoCrMo alloys [41,43].

The model considers that in a galvanic cell, the anodic current density i_a is equal to the cathodic current density i_c multiplied by the ratio of the surface area of the cathode A_c and the surface area of the anode:

$$i_a = -i_c A_c / A_a \tag{4}$$

Where i_a is the anodic current density (A/cm^2), A_a is the area of the wear track (cm^2), i_c is the cathodic current density (A/cm^2) and A_c is the area of the passive region (cm^2). In this study, the current density is assumed to be homogenous over the cathode and anode regions.

The cathode potential E_c (V) can be obtained through the Butler-Volmer equation:

$$E_c = E_{cor*} + b_c log i_{cor} - b_c log|i_c| \tag{5}$$

Where E_{cor*}, b_c and i_{cor} can be extracted from the cathodic polarization curves, as summarized in Table 2.

The OCP decay is assumed to be the same for all tested patients, with a value around 0.3 V, taken from the only research on CoCrMo alloy in NaCl and bovine serum using a simulator [23]. Similar values (0.1 - 0.35 V depending on the solution and load) were also observed using laboratory tribometers in previous works [44–46].

Considering Eq. (5), i_c values of both materials under tribocorrosion condition for all tested patients can be extracted and are shown in Fig. 10. For comparison, the i_{cor} of both materials are also present in the graph as triangles. Interestingly, the estimated cathodic current densities in Fig. 10 change significantly among patients from −0.4 μA/cm^2 (P73) to −10 μA/cm^2 (P20). This implies that one has to expect significant variations (up to a factor of 25) in the metal ion release into the body from joint implants, and this variation depends on the patient.

To assess the anodic current, i.e., the corrosion rate, it is necessary to determine the A_a and A_c values. A_c corresponds essentially to the surface area of the sample. For an artificial hip joint with a CoCrMo head diameter of 32 mm, the corresponding sphere surface area (i.e., 3217 mm^2) can be approximately taken as A_c. The anodic area can be estimated to correspond to the scratched area during a gait, i.e., the width of the plastic indentation on the metallic head multiplied by the peripheral sliding distance. By considering a CoCrMo head of 3.6 GPa hardness [47] and an average indentation force of 1500 N (according to ISO 14, 242–1 with a body weight of 75 kg), one obtains, by diving indentation force by the hardness, a contact area of 0.42 mm^2 with a diameter of 0.73 mm (assuming a circular contact area). The extension flexion range of amplitudes in adults is around 60° (1.05 rad) [48], yielding a sliding distance of 16.8 mm for a 32 mm diameter head. The scratched area (A_a) per gait cycle is thus 12 mm^2 (16.8 mm times 0.73 mm), a value much smaller (by a factor of 268) than A_c. These yields wear accelerated corrosion rates ranging from 107 (P73) to 2680 (P20) μA/cm^2. These values are significantly higher (by 3 to 4 orders of magnitude) than the corrosion rates determined under static conditions (see Fig. 11). Similar enhancement of corrosion rates by rubbing was reported in *in-vitro* tribocorrosion studies [49].

The wear-accelerated corrosion rates expressed in μA/cm^2 can be converted to the more usual unit of mm^3/s (released material volume per s or cycle for a gait frequency of 1 Hz) used in wear studies of

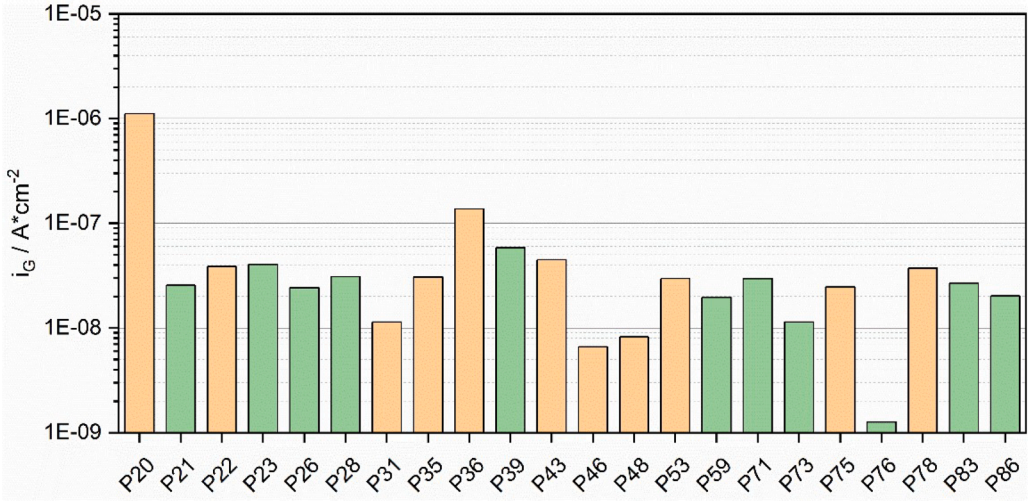

Fig. 10. Galvanic current density of Ti/CoCrMo couplings in human synovial fluids (the bars displayed in green indicate that CoCrMo alloy acts as the anode).

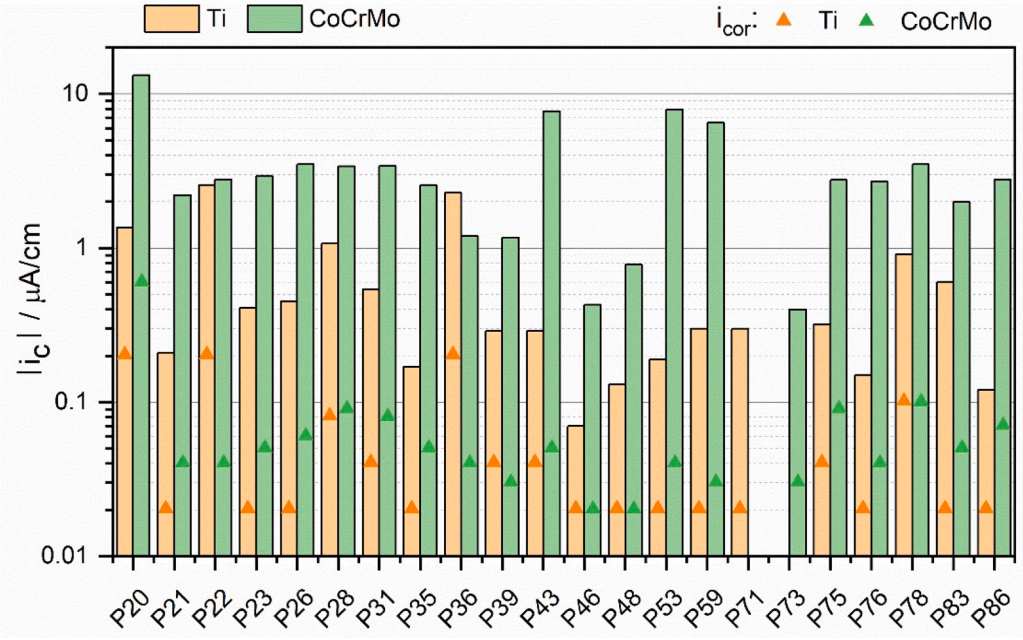

Fig. 11. i_c of Ti and CoCrMo alloy under tribocorrosion conditions for different patients (i_{cor} for both materials are displayed as triangles). Unstable OCP of CoCrMo alloy was obtained for P71.

artificial joints. Using Faraday law, one obtains material loss rates in the range of 0.24 to 6× 10^{-7} mm^3/s. These values are in line with the steady state wear rates reported from hip joint simulator studies of CoCrMo alloys (0.2 - 15× 10^{-7} mm^3/s) [50]. This good correlation supports the tribocorrosion galvanic coupling model and the possibility of assessing the variability of hip joint implants among patients by measuring the polarization behavior *in vivo*. However, the extent of wear and wear accelerated corrosion rate is also affected by the lubricating properties of the synovial fluid, i.e., on its viscosity.

5. Conclusions

In this study, the electrochemical behavior of Ti and CoCrMo alloy directly in human synovial fluids was investigated. Based on the results, conclusions can be drawn below:

- The electrochemical behavior of Ti in human synovial fluids varies significantly with patients, being several orders of magnitude different. The electrochemical behavior of CoCrMo alloy is also patient-dependent although its relative variation is sensibly less.
- The corrosion rates of Ti and CoCrMo alloy correspond to the metal ion release rates as determined by urine analyses from patients with implanted hip and knee artificial joints. This shows that the measurements taken in a short time range can be used to anticipate the long-term behavior.
- The obtained results show that no significant risk of galvanic corrosion between Ti and CoCrMo alloy occurs in human synovial fluids. This is mainly because the two metals exhibit very similar open circuit potentials once exposed to a synovial fluid.
- Through this *in-vivo* experimental protocol combined with an established tribocorrosion model, the degradation rates for hip implants (wear accelerated corrosion rates) were calculated. The calculated wear accelerated corrosion rates are much larger than the static corrosion rates, and their order of magnitude corresponds well to the data obtained from simulators. The wear rate of implants may significantly vary among patients depending on the electrochemical properties of their synovial fluid.

Funding

This work was supported by Founds National Suisse, Grant No 200021-184851/1 “Mesynic”.

CRediT authorship contribution statement

Yueyue Bao: Writing – original draft, Writing – review & editing, Methodology, Investigation, Data curation, Conceptualization. **Anna Igual Muñoz:** Writing – review & editing, Conceptualization, Supervision, Methodology, Investigation, Formal analysis, Funding acquisition. **Brigitte M. Jolles:** Supervision, Methodology, Funding acquisition, Writing – review & editing, Conceptualization. **Stefano Mischler:** Writing – review & editing, Supervision, Funding acquisition, Formal analysis, Methodology, Conceptualization.

Declaration of Competing Interest

The authors declare the following financial interests/personal relationships which may be considered as potential competing interests:

Anna Igual Munoz reports financial support was provided by Founds National Suisse. Yueyue Bao, Stefano Mischler, Brigitte M. Jolles reports financial support was provided by Founds National Suisse. If there are other authors, they declare that they have no known competing financial interests or personal relationships that could have appeared to influence the work reported in this paper.

Data availability

The authors do not have permission to share data.

Acknowledgments

The author Yueyue Bao would also like to acknowledge a grant from the China Scholarship Council.

Supplementary materials

Supplementary material associated with this article can be found, in the online version, at doi:10.1016/j.electacta.2023.143708.

References

[1] B. Bashinskaya, R.M. Zimmerman, B.P. Walcott, V. Antoci, Arthroplasty utilization in the united states is predicted by age-specific population groups, ISRN Orthop. 2012 (2012) 1–8, https://doi.org/10.5402/2012/185938.

[2] F. Pilo, D. Cilloni, M.G. Della Porta, G.L. Forni, et al., Iron-mediated tissue damage in acquired ineffective erythropoiesis disease: it's more a matter of burden or more of exposure to toxic iron form? Leuk. Res. 114 (2022) 106792 https://doi.org/10.1016/j.leukres.2022.106792.

[3] A. Lons, S. Putman, G. Pasquier, H. Migaud, et al., Metallic ion release after knee prosthesis implantation: a prospective study, Int. Orthop. 41 (2017) 2503–2508, https://doi.org/10.1007/s00264-017-3528-9 (SICOT).

[4] M. Rodríguez de la Flor, D. Hernández-Vaquero, J.M. Fernández-Carreira, Metal presence in hair after metal-on-metal resurfacing arthroplasty, J. Orthop. Res. 31 (2013) 2025–2031, https://doi.org/10.1002/jor.22450.

[5] C.W. Forsthoefel, N.M. Brown, M.L. Barba, Comparison of metal ion levels in patients with hip resurfacing versus total hip arthroplasty, J. Orthop. 14 (2017) 561–564, https://doi.org/10.1016/j.jor.2017.07.019.

[6] C. Valero Vidal, Study of the Degradation Mechanisms of the CoCrMo Biomedical Alloy in Physiological Media by Electrochemical Techniques and Surface Analysis, Universitat Politècnica de València, 2012, https://doi.org/10.4995/Thesis/10251/16881.

[7] E. Rahimi, R. Offoiach, K. Baert, H. Terryn, et al., Role of phosphate, calcium species and hydrogen peroxide on albumin protein adsorption on surface oxide of Ti6Al4V alloy, Materialia 15 (2021) 100988, https://doi.org/10.1016/j.mtla.2020.100988.

[8] Y. Tsutsumi, T. Nishisaka, H. Doi, M. Ashida, et al., Reaction of calcium and phosphate ions with titanium, zirconium, niobium, and tantalum: reaction of calcium and phosphate ions with metals, Surf. Interface Anal. 47 (2015) 1148–1154, https://doi.org/10.1002/sia.5866.

[9] I. Milošev, J. Hmeljak, A. Cör, Hyaluronic acid stimulates the formation of calcium phosphate on CoCrMo alloy in simulated physiological solution, J. Mater. Sci. Mater. Med. 24 (2013) 555–571, https://doi.org/10.1007/s10856-012-4827-8.

[10] F. Yu, O. Addison, A.J. Davenport, A synergistic effect of albumin and H_2O_2 accelerates corrosion of Ti6Al4V, Acta Biomater. 26 (2015) 355–365, https://doi.org/10.1016/j.actbio.2015.07.046.

[11] S. Karimi, T. Nickchi, A. Alfantazi, Effects of bovine serum albumin on the corrosion behaviour of AISI 316 L, Co-28Cr-6Mo, and Ti-6Al-4 V alloys in phosphate buffered saline solutions, Corros. Sci. 53 (2011) 3262–3272, https://doi.org/10.1016/j.corsci.2011.06.009.

[12] E. Liamas, O.R.T. Thomas, A.I. Muñoz, Z.J. Zhang, Effect of the electrochemical characteristics of titanium on the adsorption kinetics of albumin, RSC Adv. 9 (2019) 34265–34273, https://doi.org/10.1039/C9RA05988A.

[13] L.O. Berbel, E.D.P. Banczek, I.K. Karousis, G.A. Kotsakis, et al., Determinants of corrosion resistance of Ti-6Al-4 V alloy dental implants in an *in vitro* model of peri-implant inflammation, PLoS ONE 14 (2019) e0210530, https://doi.org/10.1371/journal.pone.0210530.

[14] N.S. More, S.N. Paul, M. Roy, Electrochemical corrosion behaviour of Ti-29Nb-13Ta-4.6Zr alloy in physiological solution containing various synovial joint lubricants, J. Bio Tribo Corros. 4 (2018) 42, https://doi.org/10.1007/s40735-018-0156-x.

[15] S. Karimi, A.M. Alfantazi, Electrochemical corrosion behavior of orthopedic biomaterials in presence of human serum albumin, J. Electrochem. Soc. 160 (2013) C206–C214, https://doi.org/10.1149/2.052306jes.

[16] S. Höhn, S. Virtanen, Effect of inflammatory conditions and H_2O_2 on bare and coated Ti–6Al–4 V surfaces: corrosion behavior, metal ion release and Ca-P formation under long-term immersion in DMEM, Appl. Surf. Sci. 357 (2015) 101–111, https://doi.org/10.1016/j.apsusc.2015.08.261.

[17] K. Szymanek, R. Charmas, W. Piasecki, A study on the mechanism of Ca^{2+} adsorption on TiO_2 and Fe_2O_3 with the usage of calcium ion-selective electrode, Chemosphere 242 (2020) 125162, https://doi.org/10.1016/j.chemosphere.2019.125162.

[18] A. Igual Munoz, J. Schwiesau, B.M. Jolles, S. Mischler, *In vivo* electrochemical corrosion study of a CoCrMo biomedical alloy in human synovial fluids, Acta Biomater. 21 (2015) 228–236, https://doi.org/10.1016/j.actbio.2015.03.008.

[19] S.G. Steinemann, Corrosion of surgical implants-*in vivo* and *in vitro* tests, in evaluation of biomaterials. Advances in Biomaterials 1980, 1–34.

[20] A.C. Lewis, M.R. Kilburn, I. Papageorgiou, G.C. Allen, et al., Effect of synovial fluid, phosphate-buffered saline solution, and water on the dissolution and corrosion properties of CoCrMo alloys as used in orthopedic implants, J. Biomed. Mater. Res. 73A (2005) 456–467, https://doi.org/10.1002/jbm.a.30368.

[21] Y. Bao, A.I. Muñoz, C.O.A. Olsson, B.M. Jolles, et al., The electrochemical behavior of Ti in human synovial fluids, Materials 15 (2022) 1726, https://doi.org/10.3390/ma15051726.

[22] M.A. Wimmer, A. Fischer, R. Büscher, R. Pourzal, et al., Wear mechanisms in metal-on-metal bearings: the importance of tribochemical reaction layers, J. Orthop. Res. (2010) 436–443, https://doi.org/10.1002/jor.21020.

[23] Y. Yan, A. Neville, D. Dowson, S. Williams, et al., Effect of metallic nanoparticles on the biotribocorrosion behaviour of metal-on-metal hip prostheses, Wear 267 (2009) 683–688, https://doi.org/10.1016/j.wear.2008.12.110.

[24] M.A. Wimmer, C. Sprecher, R. Hauert, G. Täger, et al., Tribochemical reaction on metal-on-metal hip joint bearings: a comparison between *in-vitro* and *in-vivo* results, Wear 255 (2003) 1007–1014, https://doi.org/10.1016/S0043-1648(03)00127-3.

[25] P. Zeng, A. Rana, R. Thompson, W. Rainforth, Subsurface characterisation of wear on mechanically polished and electro-polished biomedical grade CoCrMo, Wear 332-333 (2015) 650–661, https://doi.org/10.1016/j.wear.2015.02.007.

[26] R. Pourzal, R. Theissmann, S. Williams, B. Gleising, et al., Subsurface changes of a MoM hip implant below different contact zones, J. Mech. Behav. Biomed. Mater. 2 (2009) 186–191, https://doi.org/10.1016/j.jmbbm.2008.08.002.

[27] A. Igual-Munoz, J.L. Genilloud, B.M. Jolles, S. Mischler, Influence of different sterilization methods on the surface chemistry and electrochemical behavior of biomedical alloys, Bioengineering 10 (2023) 749, https://doi.org/10.3390/bioengineering10070749.

[28] D. Landolt, Corrosion and Surface Chemistry of Metals, 0 ed., EPFL Press, 2007.

[29] M.E.P. Souza, L. Lima, C.R.P. Lima, C.A.C. Zavaglia, et al., Effects of pH on the electrochemical behaviour of titanium alloys for implant applications, J. Mater. Sci. Mater. Med. 20 (2009) 549–552, https://doi.org/10.1007/s10856-008-3623-y.

[30] A. Robin, J.P. Meirelis, Influence of fluoride concentration and ph on corrosion behavior of titanium in artificial Saliva, J. Appl. Electrochem. 37 (2007) 511–517, https://doi.org/10.1007/s10800-006-9283-z.

[31] N.S. Manam, W.S.W. Harun, D.N.A. Shri, S.A.C. Ghani, et al., Study of corrosion in biocompatible metals for implants: a review, J. Alloys Compd. 701 (2017) 698–715, https://doi.org/10.1016/j.jallcom.2017.01.196.

[32] C.V. Vidal, A.I. Muñoz, C.O.A. Olsson, S. Mischler, Passivation of a CoCrMo PVD alloy with biomedical composition under simulated physiological conditions studied by EQCM and XPS, J. Electrochem. Soc. 159 (2012) C233–C243, https://doi.org/10.1149/2.090205jes.

[33] Y. Bao, T. Kudo, S. Cao, A. Igual Munoz, et al., Passivation charge density of CoCrMo alloy in different aqueous solutions, J. Bio Tribo Corros. 6 (2020) 1–10, https://doi.org/10.1007/s40735-020-00354-x.

[34] C. Valero Vidal, A. Olmo Juan, A. Igual Muñoz, Adsorption of bovine serum albumin on CoCrMo surface: effect of temperature and protein concentration, Colloids Surf. B Biointerfaces 80 (2010) 1–11, https://doi.org/10.1016/j.colsurfb.2010.05.005.

[35] C. Valero Vidal, A. Igual Muñoz, Electrochemical characterisation of biomedical alloys for surgical implants in simulated body fluids, Corros. Sci. 50 (2008) 1954–1961, https://doi.org/10.1016/j.corsci.2008.04.002.

[36] H. Matusiewicz, Potential release of *in vivo* trace metals from metallic medical implants in the human body: from ions to nanoparticles - a systematic analytical review, Acta Biomater. 10 (2014) 2379–2403, https://doi.org/10.1016/j.actbio.2014.02.027.

[37] F.M.S. Soares, C.N. Elias, E.S. Monteiro, M.E.R. Coimbra, et al., Galvanic corrosion of Ti dental implants coupled to CoCrMo prosthetic component, Int. J. Biomater. (2021), https://doi.org/10.1155/2021/1313343.

[38] H. Geng, D. Zhang, K. Chen, Q. Wang, Galvanic corrosion behavior between Ti6Al4V and CoCrMo alloys in saline solution, Mater. Express 4 (2014) 213–220, https://doi.org/10.1166/mex.2014.1163.

[39] A. Mellado-Valero, A. Muñoz, V. Pina, M. Sola-Ruiz, Electrochemical behaviour and galvanic effects of titanium implants coupled to metallic suprastructures in artificial saliva, Materials 11 (2018) 171, https://doi.org/10.3390/ma11010171.

[40] S. Mischler, Triboelectrochemical techniques and interpretation methods in tribocorrosion: a comparative evaluation, Tribol. Int. 41 (2008) 573–583, https://doi.org/10.1016/j.triboint.2007.11.003.

[41] S. Mischler, A.I. Muñoz, Wear of CoCrMo alloys used in metal-on-metal hip joints: a tribocorrosion appraisal, Wear 297 (2013) 1081–1094, https://doi.org/10.1016/j.wear.2012.11.061.

[42] A.C. Vieira, L.A. Rocha, N. Papageorgiou, S. Mischler, Mechanical and electrochemical deterioration mechanisms in the tribocorrosion of Al alloys in NaCl and in $NaNO_3$ solutions, Corros. Sci. 54 (2012) 26–35, https://doi.org/10.1016/j.corsci.2011.08.041.

[43] N. Papageorgiou, S. Mischler, Electrochemical simulation of the current and potential response in sliding tribocorrosion, Tribol. Lett. 48 (2012) 271–283, https://doi.org/10.1007/s11249-012-0022-9.

[44] R. Alonso Gil, A. Igual Muñoz, Influence of the sliding velocity and the applied potential on the corrosion and wear behavior of HC CoCrMo biomedical alloy in simulated body fluids, J. Mech. Behav. Biomed. Mater. 4 (2011) 2090–2102, https://doi.org/10.1016/j.jmbbm.2011.07.008.

[45] Y. Yan, A. Neville, D. Dowson, Biotribocorrosion-an appraisal of the time dependence of wear and corrosion interactions: I. The role of corrosion, J. Phys. D Appl. Phys. 39 (2006) 3200–3205, https://doi.org/10.1088/0022-3727/39/15/S10.

[46] A. Iwabuchi, J.W. Lee, M. Uchidate, Synergistic effect of fretting wear and sliding wear of co-alloy and Ti-alloy in Hanks' solution, Wear 263 (2007) 492–500, https://doi.org/10.1016/j.wear.2007.01.102.

[47] S. Cao, A.I. Muñoz, S. Mischler, Rationalizing the *in vivo* degradation of metal-on-metal artificial hip joints using tribocorrosion concepts, Corrosion 73 (2017) 1510–1519, https://doi.org/10.5006/2514.

[48] A.P. Sah, How much hip motion is used in real-life activities? Assessment of hip flexion by a wearable sensor and implications after total hip arthroplasty, J. Arthroplast. 37 (2022) S871–S875, https://doi.org/10.1016/j.arth.2022.03.052.
[49] A. Igual Muñoz, S. Mischler, Effect of the environment on wear ranking and corrosion of biomedical CoCrMo alloys, J. Mater. Sci. Mater. Med. 22 (2011) 437–450, https://doi.org/10.1007/s10856-010-4224-0.
[50] S. Cao, S. Mischler, Assessment of a recent tribocorrosion mdel for wear of metal-on-metal hip joints: comparison between model predictions and simulator results, Wear 362-363 (2016) 170–178, https://doi.org/10.1016/j.wear.2016.05.025.